Journal of Catalysis **205,** 375–381 (2002)
doi:10.1006/jcat.2001.3460, available online at http://www.idealibrary.com on IDEAL®

Alumina-Supported Copper Chloride

4. Effect of Exposure to O_2 and HCl

G. Leofanti,*,[1] A. Marsella,* B. Cremaschi,* M. Garilli,* A. Zecchina,† G. Spoto,† S. Bordiga,† P. Fisicaro,† C. Prestipino,† F. Villain,‡,§ and C. Lamberti†,¶,[2]

*European Vinyls Corporation Italia, Inovyl Technological Centre, Via della Chimica 5, 30175 Porto Marghera (Venezia), Italy; †Università di Torino, Dipartimento di Chimica Inorganica, Chimica Fisica e Chimica dei Materiali, Via P. Giuria 7, 10125 Torino, Italy; ‡Laboratoire de Chimie Inorganique et Matériaux Moléculaires ESA, CNRS 7071, Case 42, Bâtiment F74, Université Pierre et Marie Curie, 4 Place Jussieu, F-75252, Paris, France; §LURE, Bât. 209D, Centre Universitaire, B.P. 34, 91898 Orsay Cedex, France; and ¶Unità INFM Torino-Università

Received August 3, 2001; revised November 1, 2001; accepted November 1, 2001; published online January 3, 2002

A complete catalytic cycle was performed on $CuCl_2/Al_2O_3$ catalyst for ethylene oxychlorination at 500 K. X-ray absorption near-edge spectroscopy, extended X-ray absorption fine structure, electron paramagnetic resonance, and IR of adsorbed CO were used to demonstrate that the ethylene oxychlorination reaction, $C_2H_4 + 2HCl + 1/2\,O_2 \rightarrow C_2H_4Cl_2 + H_2O$, follows a three-step mechanism: (i) reduction of $CuCl_2$ to CuCl ($2CuCl_2 + C_2H_4 \rightarrow C_2H_4Cl_2 + 2CuCl$), (ii) oxidation of CuCl to give an oxychloride ($2CuCl + 1/2\,O_2 \rightarrow Cu_2OCl_2$), and (iii) closure of the catalytic circle by rechlorination with HCl, restoring the original $CuCl_2$ ($Cu_2OCl_2 + 2HCl \rightarrow 2CuCl_2 + H_2O$). The dispersing/sintering effect of the different reagents on the active phase has been also investigated.

Key Words: **Al_2O_3-supported $CuCl_2$; ethylene oxychlorination; IR spectroscopy; EPR; XANES; EXAFS.**

1. INTRODUCTION

Nowadays, almost all the world's production of vinyl chloride is based on cracking of 1,2-dichloroethane, which in turn is produced by catalytic oxychlorination of ethylene with hydrochloric acid and oxygen (1) following the reaction path

$$C_2H_4 + 2HCl + 1/2\,O_2 \rightarrow C_2H_4Cl_2 + H_2O. \qquad [1]$$

The reaction is performed at 490–530 K and 5–6 atm (1 atm $\approx 1.01 \times 10^5$ Pa) using both air and oxygen in fluid or fixed-bed reactors (2). Commercial catalysts are produced by impregnation of alumina with $CuCl_2$ (4–8 wt% Cu). Other chlorides (mainly alkaline or alkaline earth chlorides) in a variable concentration (1, 3) are also added in order to improve the catalytic performances, making the catalyst more suitable for use in industrial reactors (1, 3, 4).

This paper represents the last part of a series devoted to the investigation of the base catalyst (i.e., $CuCl_2$ supported on γ-alumina) (5–8). The first works (5–7) were devoted to a study of the catalyst before interaction with reagents. It was demonstrated that two copper species are present on the catalyst activated in N_2 flux at the reaction temperature (500 K), just before reagent feeding. The former is a surface Cu aluminate phase where Cu(II) occupies the octahedral cationic vacancies of γ-alumina and the latter is an amorphous, highly dispersed $CuCl_2$ phase. The copper surface aluminate phase is the only one present on the low loaded samples. At a concentration higher than 0.95 wt% Cu per 100 m^2 of support, it coexists with the $CuCl_2$, which is the only active phase.

The oxychlorination reaction [1] has been supposed to occur in three subsequent steps (8–14): (i) reduction of $CuCl_2$ into CuCl by ethylene, (ii) reoxidation of CuCl by oxygen, and (iii) closure of the loop, by restoration of the original $CuCl_2$, with HCl, as described in Eqs. [2]–[4]:

$$2CuCl_2 + C_2H_4 \rightarrow C_2H_4Cl_2 + 2CuCl, \qquad [2]$$

$$2CuCl + 1/2\,O_2 \rightarrow Cu_2OCl_2, \qquad [3]$$

$$Cu_2OCl_2 + 2HCl \rightarrow 2CuCl_2 + H_2O. \qquad [4]$$

Step [2] has recently been the object of work devoted to the study of the interaction of the catalysts with ethylene (8), which has demonstrated its effective occurrence. Conversely, no experimental evidence of steps [3] and [4] has been reported up to now. The present work is devoted to the study of the interactions with O_2 and HCl. However, some results obtained on the catalyst after exposure to ethylene are also be reported, for better understanding.

[1] Current address: Via Firenze 43, 20010 Canegrate (Milano), Italy.
[2] To whom correspondence should be addressed. Fax: +39-011-6707855. E-mail: Lamberti@ch.unito.it.

0021-9517/02 $35.00

2. EXPERIMENTAL

A $CuCl_2/Al_2O_3$ catalyst (Cu 7.5 wt%, hereafter labeled Cu7.5) was prepared by impregnation of γ-alumina (Condea Puralox SCCa 30/170; surface area, 168 $m^2\,g^{-1}$, pore volume, 0.50 $cm^3\,g^{-1}$) with an aqueous solution of $CuCl_2$ following the incipient wetness method (5). The treatment temperature, for both sample activation and interaction with reagents, was 500 K. The interaction with HCl was further investigated at 600 K.

For IR measurements, performed at room temperature (RT), a thin, self-supporting wafer of the catalyst was prepared and activated under dynamic vacuum at 500 K for 2 h, inside an IR cell designed to allow *in situ* temperature treatments, reagent dosage and evacuation, and CO dosage. The IR spectra were recorded at 2-cm^{-1} resolution on a BRUKER Fourier transform IR (FTIR) 66 spectrometer equipped with a mercury cadmium telluride cryodetector.

Electron paramagnetic resonance (EPR) spectra were measured at liquid nitrogen temperature (LNT) on a Varian E 109 spectrometer equipped with a dual cavity and operating in the X band. Varian Pitch was used as a reference for the calibration of g values. Before cooling, the samples were evacuated at RT up to 10^{-3} Torr (1 Torr $\approx$ 133.3 Pa).

X-ray absorption measurements were carried out using synchrotron radiation of the EXAFS13 station at LURE (Orsay, France) during experiment CK017-00 (XAFS13, D42, September 11–15, 2000). All details concerning data acquisition have been reported in Ref. (8). $\chi(k)$ extraction and extended X-ray absorption fine structure (EXAFS) data analysis were performed using programs developed by Michalowicz (15), following standard procedures (16), as described in detail in Ref. (17). The Cu–Cl and Cu–O phase shift and amplitude functions were extracted from anidrous $CuCl_2$ [four equivalent chlorine atoms at 2.26 Å (18)] and from Cu_2O [four equivalent oxygens at 1.85 Å (19)] model compounds assuming arbitrarily a relative Debye-Waller factor σ of 4.0 and 5.0×10^{-2} Å, respectively. The fitting of the EXAFS data was performed in k-space on the $k\chi(k)$ function, as described in Ref. (15). The fits reported hereafter (vide infra Figs. 5b and 6b) correspond to the minimized functions.

3. RESULTS

3.1. IR Study of Adsorbed CO at RT

CO is an excellent probe molecule for surface Cu(I) sites because its interaction is normally rather strong (20). In contrast, its interaction with Cu(II), sites is very weak (21) and can be considered, as a first approximation, negligible in RT experiments. In the case of the $CuCl_2/Al_2O_3$ catalysts, as demonstrated in Ref. (8), Cu(I)···CO species are the unique adducts observed on dosing CO at RT, being carbonyl adducts formed on the support (Al^{3+}···CO and Al–OH···CO) observed at LNT only. As a consequence, the intensity of the C–O stretching band, at a given P_{CO}, can be roughly correlated to the amount of Cu(I) sites available at the surface of the catalysts (8).

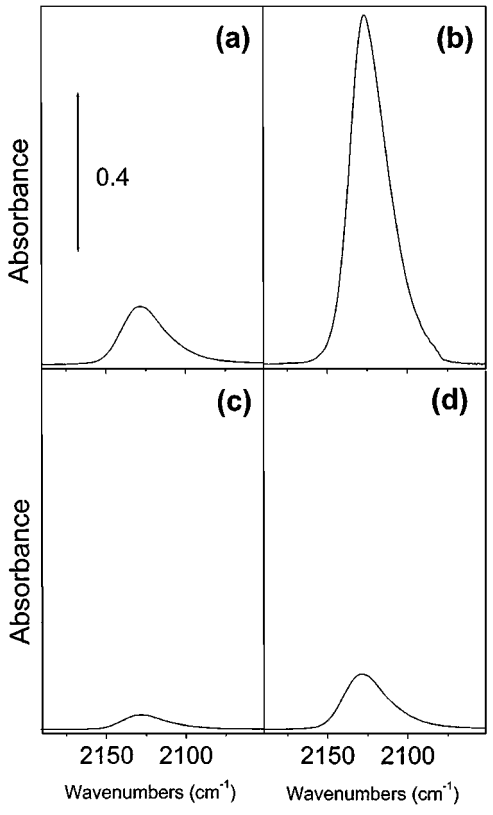

FIG. 1. IR spectra collected on dosing CO (40 Torr) at RT on Cu7.5 catalyst along the catalytic path foreseen in Eqs. [2]–[4]. Activated sample (a) and after interaction with C_2H_4 (b), O_2 (c), and HCl (d). These data mirror the number of surface Cu^+ ions.

Figure 1 shows the IR spectra of CO dosed at RT (P_{CO} = 40 Torr) on a Cu7.5 sample along the catalytic path foreseen in Eqs. [2]–[4]. Interaction with C_2H_4, step 1, causes a strong increase in the C–O stretching band (compare Figs. 1a and 1b). Interaction with oxygen, step 2, causes the opposite reaction (Fig. 1c vs Fig. 1b), while interaction with HCl, step 3, results in restoration of the initial spectrum (Fig. 1d vs Fig. 1a).

3.2. EPR Study

Because the electronic configurations of Cu(I) and Cu(II) ions are d^{10} and d^9, respectively, only the latter is involved in EPR spectroscopy and thus the integrated value of the EPR signal can be considered proportional, as a first approximation, to the amount of isolated Cu(II) (8, 22, 23).

Figure 2 reports the integrated area of the EPR signal measured on catalyst Cu7.5 after activation at RT, at 500 K, and along the catalytic path foreseen in Eqs. [2]–[4]. The

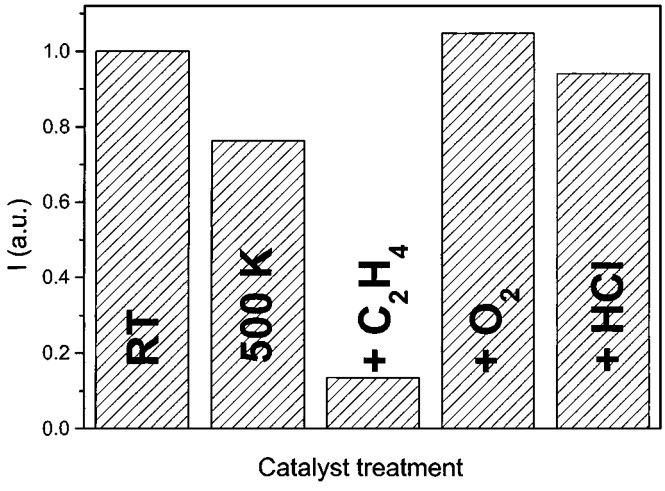

FIG. 2. Integrated signal extracted from the EPR spectra collected at 77 K on Cu7.5 catalyst along the catalytic path. Sample activated at RT, at 500 K, and after interaction with C_2H_4, O_2, and HCl. The value obtained on the catalyst activated at RT was arbitrarily set to 1.0. These data qualitatively mirror the number of Cu^{2+} ions.

integrated value obtained from the first spectrum was arbitrarily set to 1.0. The evolution of the integrated EPR signal can be summarized as follows: (i) activation at 500 K implies a partial decrement of the signal; (ii) interaction with ethylene causes a further decrement; (iii) interaction with O_2 yields to a value even higher than the original one; and (iv) finally, interaction with HCl brings the signal back to a value very close to the original one.

3.3. *XANES Study*

As extensively discussed in (8), XANES spectroscopy is sensitive to both oxidation and coordination states of Cu. The position of the Cu *k*-edge is mainly determined by the oxidation state of copper, occurring for Cu(I) species at 4–6 eV below that measured for Cu(II) species. A variation of the coordination sphere results in a less relevant edge shift and in a consistent modification of the near-edge structures.

Figures 3a–3c show the progressive evolutions undergone by the XANES spectrum of the Cu7.5 catalyst following the sequence described in Eqs. [2]–[4]. Interaction with ethylene implies a redshift of the edge from ≈8984 to ≈8979 eV (Fig. 3a), while an opposite shift is observed after interaction with O_2 (Fig. 3b). Interaction with HCl does not modify appreciably the edge position but causes a modification of the near-edge features, both of white-line intensity and first-oscillations shape.

If the rechlorination experiment is performed at a higher temperature (600 K) the XANES spectrum of the catalyst becomes very close in appearance to that of the anhydrous $CuCl_2$ model compound (Fig. 3d). A so-remarkable similarity between the two spectra shown in Fig. 3d indicates that treatment in HCl at 600 K removes, at least partially, Cu^{2+} ions from the γ-Al_2O_3 surface. This fact can be potentially confirmed by EXAFS (vide infra Fig. 6 and Table 1); however, due to its very low Debye–Waller parameter, the Cu–Cl shell dominates the EXAFS signal and, so, the fraction of Cu^{2+} ions remaining on the γ-Al_2O_3 surface cannot be quantitatively determined.

3.4. *EXAFS Study*

EXAFS spectroscopy has been a key technique in the determination of the substitution of O with Cl (or vice versa) in the first coordination sphere of copper species present in the $CuCl_2/Al_2O_3$ catalyst during aging, heating, and interaction with ethylene (5–8). In fact, the Cu–O contribution gives rise, in the uncorrected FT phase, to a peak in the 1.5-Å zone, while Cu–Cl results in a peak at around 1.9 Å. Moreover, the Cu–O phase is shifted to about π, with respect to the Cu–Cl phase, along nearly all the *k* region of interest, which makes easier the recognition of the two contributions (5, 6).

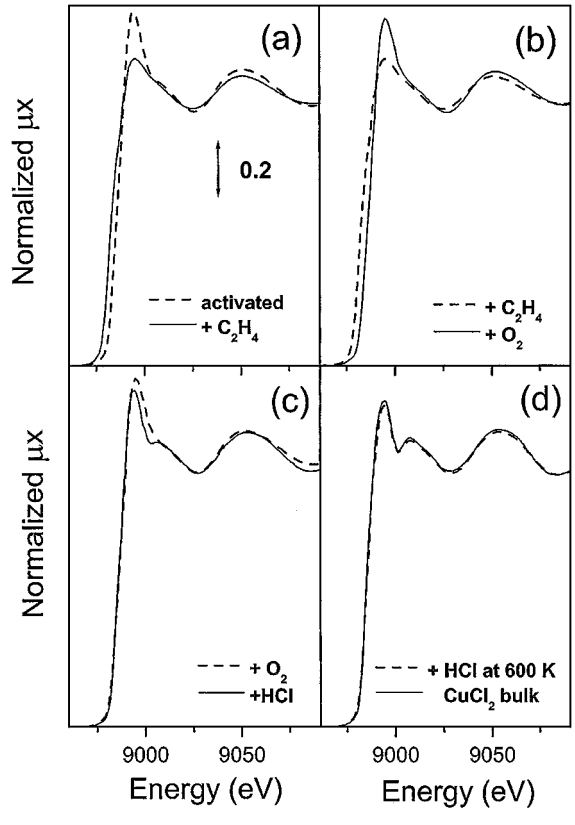

FIG. 3. (a–c) Evolution of the XANES spectra of the Cu7.5 catalyst along the catalytic path at 500 K. (a) Effect of exposure to C_2H_4; (b) effect of exposure to O_2; (c) effect of exposure to HCl. Dashed and solid lines refer to the sample before and after the treatment respectively. (d) The spectrum of the catalyst after successive interaction with HCl at 600 K (dashed line) compared with that of the bulk anhydrous $CuCl_2$ model compound.

TABLE 1

Filtering Ranges and EXAFS Results for First Coordination Sphere of the γ-Al_2O_3-Supported $CuCl_2$ Catalysts [a]

Catalyst	Δk (Å^{-1})	ΔR (Å)	Scatter	R (Å)	N	σ (10^{-2} Å)	ΔE (eV)	ρ
Cu1.4[b]	3.34–14.31	1.07–1.84	Cu–O	1.94 ± 0.01	4.98 ± 0.25	5.8 ± 0.6	-1 ± 2	5×10^{-4}
Cu7.5 activated	2.93–14.09	0.92–2.30	Cu–O	1.94	1.07	5.8	-1	6×10^{-3}
			Cu–Cl	2.25 ± 0.02	3.15	7.0 ± 1	-1 ± 2	
Cu7.5 + C_2H_4	2.93–14.09	0.90–2.34	Cu–O	1.94	1.07	5.8	$+3 \pm 2$	7×10^{-3}
			Cu–Cl	2.25 ± 0.02	3.15	8.4 ± 1.3	-1 ± 2	
Cu7.5 + O_2	2.93–14.09	0.84–2.34	Cu–O	1.94	1.07	5.8	-1	
			Cu–O	1.93 ± 0.02	1.7 ± 0.3	7.3 ± 1	-1 ± 2	2×10^{-3}
			Cu–Cl	2.26 ± 0.02	2.0 ± 0.3	5.6 ± 1	-1 ± 2	
Cu7.5 + HCl	2.93–14.09	0.90–2.30	Cu–O	1.94	1.07	5.8	-1	8×10^{-3}
			Cu–Cl	2.24 ± 0.02	3.15	7.4 ± 1	-1 ± 2	
Cu7.5 + HCl at 600 K	2.93–14.09	0.90–2.30	Cu–Cl	2.26 ± 0.02	4.0	4.2 ± 0.7	-2 ± 2	1×10^{-4}

[a] Δk, Interval of k-space to R-space FT; ΔR, R-space interval selected to perform the first shell-filtered back FT into k-space; R, bond distance; N, coordination number; σ, relative Debye–Waller factor; ΔE, energy shifts. Nonoptimized parameters can be discriminated by the absence of the corresponding error bars. The last column reports the quality factor of the fit (ρ) computed as detailed in Ref. (15b).

[b] The fit of the Cu1.4 catalyst, containing only the surface Cu aluminate phase, has been reproduced from Ref. (8) for comparison.

Figure 4a reports the evolution of the modulus of the FT of the $\chi(k)$ function along the foreseen catalytic path. The effect of interaction with ethylene is discussed in Ref. (8), to which the reader is directed for details. Here only the FT (solid line curve in Fig. 4a) is reported in order to appreciate the effect of the subsequent interaction with O_2 (dashed line curve). Besides an overall increase in the EXAFS signal, the relative increase in the low-R component in the first shell around copper is evident. The subsequent interaction with HCl has the opposite effect, causing an increase in the high-R component, to the detriment of the low-R one.

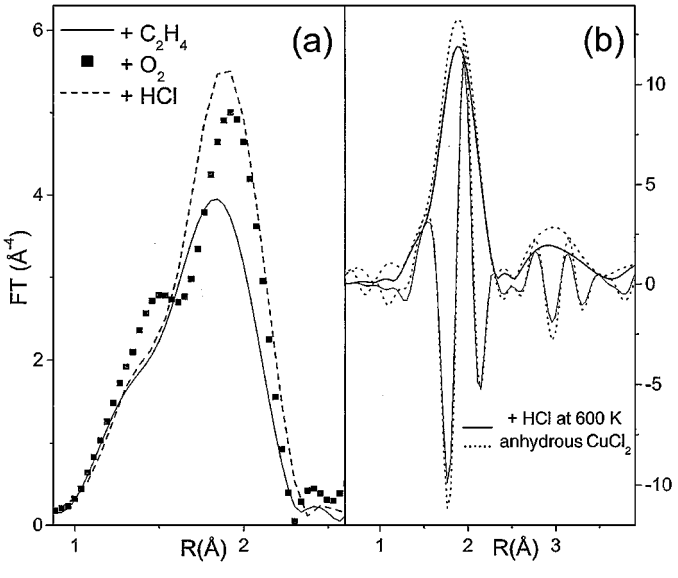

FIG. 4. (a) Evolution of the modulus of the phase-uncorrected, k^3-weighted FT of the EXAFS function along the catalytic path. (b) The Cu7.5 catalyst after interaction with HCl at 600 K (dotted line) compared with the bulk anhydrous $CuCl_2$ model compound (solid line).

As in the case of the XANES spectrum (Fig. 3d), if the rechlorination experiment is performed at a higher temperature (600 K), the FT of the EXAFS spectrum of the catalyst also becomes close in appearance to that of the anhydrous $CuCl_2$ model compound (Fig. 4b).

4. DISCUSSION

It has already been proved (8) that interaction with ethylene causes reduction of the $CuCl_2$ phase to CuCl following reaction [2], while the Cu aluminate phase does not participate in the process and remains unchanged. It has been also shown that the interaction of dispersed $CuCl_2$ with ethylene results in CuCl particles characterized by an even higher dispersion.

4.1. Interaction with O_2

The results reported in Section 3 give direct evidence of the oxidation of Cu(I) to Cu(II) as an effect of the exposure of the catalyst to O_2. In fact, (i) IR spectroscopy singles out a significant decrease in the C–O stretching band, attributed to the Cu(I)···CO adducts (Fig. 1c vs Fig. 1b), (ii) EPR spectroscopy shows an increase in the integrated area of the Cu(II) signal [the decrease in the EPR signal observed in the activation of the catalyst at 500 K is explained in Ref. (8) in terms of a partial Cu(II) → Cu(I) reduction caused by the thermal treatment], and (iii) XANES data (Fig. 3b) are characterized by a blueshift of 5 eV. In particular, XANES testifies to the nearly complete (both surface and bulk) Cu(I) → Cu(II) oxidation. It can be concluded that the copper species present on the catalyst after interaction with oxygen are in the oxidation state +2, which is in agreement with the reaction path hypothesized in Eq. [3].

Proof of the insertion of oxygen ligands in the first coordination shell of copper is supplied by EXAFS spectroscopy.

From a first view of the data reported in Fig. 4a (dashed line vs solid one), the relative increase in the low-R tail of the first shell peak (around 1.45 Å without phase correction) is evident. It can so be qualitatively concluded that interaction with O_2 results in a relative increase in the Cu–O contribution with respect to the Cu–Cl one.

To obtain quantitative results, a detailed EXAFS data analysis must be done. To explain the procedure followed to analyze the spectrum of the oxidized catalyst, a summary of the analogous analysis done on the activated catalyst, before and after interaction with C_2H_4 (8), is useful. According to Refs. (5–7), the activated Cu7.5 catalyst has 1.6 Cu wt% as surface copper alumnate and the remaining 5.9 Cu wt% as dispersed copper chloride, resulting in relative percentages of 21 and 79%, respectively. Copper ions in the surface aluminate phase occupy the octahedral cationic vacancies of γ-alumina and exhibit a first coordination shell formed by five oxygen ligands located at 1.94 Å (8). The results are reported in the first row of Table 1 for comparison. Copper ions of the dispersed copper chloride phase are supposed to have a first coordination close to that observed for bulk chloride in diffraction studies [i.e., four chlorine atoms at 2.26 Å (18)]. The EXAFS signal of the activated Cu7.5 catalyst before and after exposure to ethylene has been successfully modeled (8) as the sum of 21% ($N_{Cu-O} = 1.07$, instead of 5) of the EXAFS signal of the surface Cu aluminate phase and of 79% ($N_{Cu-Cl} = 3.15$, instead of 4) of the copper chloride phase, optimizing only four parameters (two ΔE, the R_{Cu-Cl}, and σ_{Cu-Cl}: second and third catalysts in Table 1).

The same procedure was applied to the catalyst after interaction with O_2, by supposing that 21% of the overall signal was still coming from the unperturbed Cu aluminate phase and that the remaining 79% was coming from a chemically undefined oxychloride showing both Cl and O atoms in the first coordination shell of copper. The optimization of the EXAFS data based on this model requires the simultaneous refinement of eight parameters (R, N, σ, and ΔE for both the Cu–O and the Cu–Cl shells of the oxychloride phase). [Once determined for in the Cu1.4 catalyst (8), the structural parameters (R, N, σ) of the Cu aluminate phase were kept fixed along the catalytic path of the Cu7.5 catalyst. In the cases where the copper present on the sample was in the oxidation state +2 (after activation and interaction with O_2 and HCl), the $\chi(k)$ extraction was done using the same E_0 as was used for the Cu1.4 catalyst: this allowed us to fix also ΔE to –1 eV. Only in the case of Cu7.5 catalyst after interaction with C_2H_4 was ΔE optimized because, in that case, the catalyst was the Cu–K edge 5 eV downward shifted and a different E_0 had to be adopted. A difference of 4 eV (the expected value being 5 eV) was found in that case for the ΔE value of the Cu aluminate phase.] With $2\Delta k \Delta R/\pi$ close to 10 (Table 1), an eight-parameter fit is allowed (16). The quantitative result of the fit is reported in Table 1, while the quality of the fit can be seen in Figs. 5a and 5b in the k and R spaces, respectively. With Cu_2OCl_2 the tentative oxychloride used in Eq. [3], the quantitative EXAFS results are compared with the structural data available in the literature for bulk Cu_2OCl_2, where copper has a first coordination shell formed by two oxygen atoms at 1.94 Å and two chlorine atoms at 2.29 Å (24). The Cu–O distance obtained in the EXAFS fit (1.93 ± 0.02) is very close to the crystallographic value, while the Cu–Cl distance is 0.03 Å less (2.26 ± 0.02) (see Table 1). Coming to N, values of 1.7 ± 0.3 and 2.0 ± 0.3 have been obtained from the fit for oxygen and chlorine, respectively. As discussed in detail in Ref. (8), when more than a Cu phase is present on the samples, the N values obtained from the EXAFS fit are not the *true* coordination numbers but are only proportional to them. The proportionality constant is the inverse of the relative fraction of the phase. In the present case the constant is 1.27 for the oxychloride phase, resulting in estimated *true* coordination numbers of 2.2 ± 0.4 and 2.5 ± 0.4 for oxygen and chlorine, respectively. Even if slightly overestimated, the obtained coordination number for oxygen and chlorine are, within the error bars, compatible with the bulk structure of Cu_2OCl_2. However, the formation of other Cu oxychlorides of different stoichiometry can not be safely ruled out owing to the average nature of the data determined by EXAFS spectroscopy and to the relative high error bars associated with the coordination numbers.

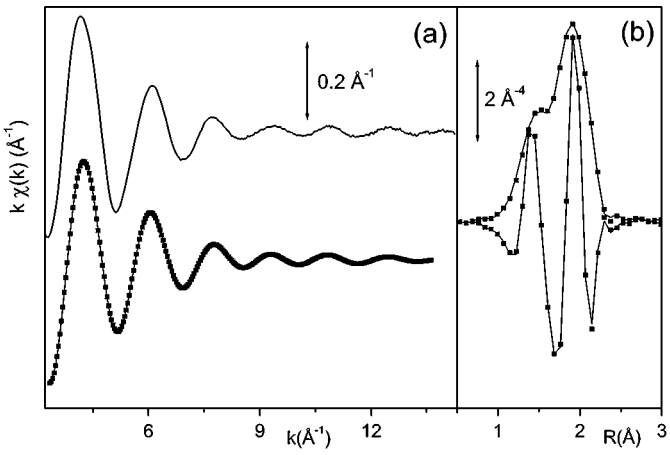

FIG. 5. (a) Catalyst Cu7.5 after interaction with O_2: raw EXAFS spectrum and corresponding first-shell filtered signal, superimposed on its theoretical simulation. (b) k^3-weighted, phase-uncorrected FT of both experimental and theoretical curves (modulus and imaginary parts).

Using EXAFS the insertion of oxygen atoms into the first coordination shell of copper atoms of the active phase is thus evident. This is direct proof that an oxychloride, as foreseen in Eq. [3], has been formed in the active phase of the catalyst. Cu_2OCl_2 is a good candidate, being that both bond distances and coordination numbers obtained in the EXAFS fit are compatible with the crystallographic values.

The effect of exposure to O_2 on the dispersion of the active phase can be monitored using EXAFS. The interaction with O_2 results in an overall increase in the EXAFS signal, moving the magnitude of the first shell peak (Fig. 4a) from 4 to 5 $Å^{-4}$. The increase is justified by a decrease in the σ_{Cu-Cl} Debye–Waller factor from 8.4 to 5.6×10^{-2} Å (Table 1), which can be interpreted as a sintering caused by interaction with O_2, opposite the desegregation induced by C_2H_4, evidenced by the increase in σ_{Cu-Cl} from 7.0 to 8.4 $\times$ 10^{-2} Å (8).

4.2. Interaction with HCl

The results reported in Section 3 can be used to demonstrate the fact that the oxidation state of copper does not change on exposure to HCl. The XANES data of the Cu7.5 catalyst after interaction with O_2 and HCl, reported in Fig. 3c, show that no measurable edge shift occurs on interaction with HCl, indicating that the oxidation state of copper species still remains +2. The substantial invariance of the integrated intensity, detectable on both IR (Figs. 1a and 1d) and EPR (Fig. 2) data, confirms that we are dealing with cupric ions.

The change caused by interaction with HCl concerns the coordination sphere of Cu: the phenomenon is pointed out by an alteration in the near-edge structure, particularly in the 8990–9010 eV range. A more consistent proof comes from EXAFS.

In this case, following the hypothesis that all the active phase is again in the form of anhydrous $CuCl_2$, the EXAFS signal has been simulated in terms of two components only: 21% of surface aluminate and 79% of $CuCl_2$. All parameters of the first contribution have been fixed ($N_{Cu-O} = 1.07$, $\Delta E = -1$ eV, $R_{Cu-O} = 1.94$ Å, and $\sigma_{Cu-Cl} = 5.8\ 10^{-2}$ Å); the same holds for $N_{Cu-Cl} = 3.15$. So the fit runs only on the remaining parameters of the copper chloride phase (ΔE, R_{Cu-Cl}, and σ_{Cu-Cl}). The three-parameter fit (Table 1) yields, within the experimental error, the expected R_{Cu-Cl} distance (2.24 ± 0.02 vs 2.26 Å), and reasonable values for both ΔE and σ_{Cu-Cl} parameters, supporting the validity of our hypothesis. The dispersion of the $CuCl_2$ particles obtained by interaction with HCl is still rather high, being the optimized σ_{CuCl} of 7.4×10^{-2} Å, a value to be compared with 7.0×10^{-2} Å of the activated sample. We can conclude that the final product is anhydrous $CuCl_2$; thus the final step ($Cu_2OCl_2 + 2HCl \rightarrow 2CuCl_2 + H_2O$) of the catalytic cycle has been proven.

If the temperature of interaction with HCl is increased from 500 to 600 K, a remarkable sintering effect is obtained on the $CuCl_2$. In fact, the intensity of the EXAFS signal doubles, as a consequence of a strong decrease in the static part of the Debye–Waller factor (see Fig. 4). Moreover, XANES data (vide supra Fig. 3d and related comments) indicate that treatment in HCl at 600 K partially removes Cu^{2+} ions from the γ-Al_2O_3 surface. Both phenomena make the XANES

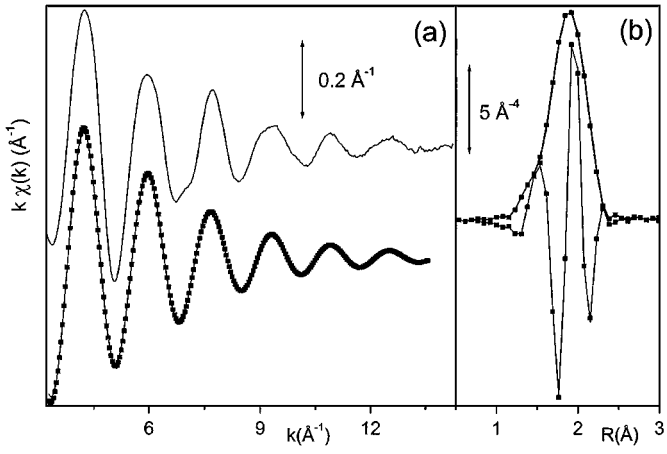

FIG. 6. As for Fig. 5 for catalyst Cu7.5 after interaction with HCl at 600 K.

(Fig. 3d) and the EXAFS (Fig. 4b) spectra of the catalyst nearly identical to that of anhydrous $CuCl_2$ model compound. On these bases, a single shell fit has been performed on the EXAFS data (last catalyst in Table 1), obtaining the expected R_{Cu-Cl} distance (2.26 ± 0.02 Å) and an optimized σ_{CuCl} of 4.2×10^{-2} Å, very close to the value adopted for the bulk (4.0×10^{-2} Å). The quality of the fit can be seen in Figs. 6a and 6b for the *k* and *R* spaces, respectively. We have tried to quantify the fraction of Cu^{2+} ions still present on the γ-Al_2O_3 surface by adding the Cu–O contribution of the copper aluminate phase to the previous fit, as was done for the sample after interaction with ethylene and oxygen. Since the fit did not improve significantly, we must conclude that the fraction of copper on the alumina surface is below the detection capability of the technique, since the Cu–Cl shell dominates the EXAFS signal.

According to the increased size of the $CuCl_2$ crystals supported on γ-alumina, a second shell signal is now well visible in the 2.5–3.5 Å region of the FT of the EXAFS spectrum (see Fig. 4b).

These findings imply that the Cu^{2+} ions of the surface aluminate phase, which has been proved to be inactive in the ethylene conversion at 500 K (6), can be converted into the active $CuCl_2$ phase on interaction with HCl at 600 K. The following path can be hypothesized:

$$(>\text{Al-O})_2\text{Cu} + 4\text{HCl} \rightarrow \text{CuCl}_2 + 2(>\text{Al-Cl}) + 2\text{H}_2\text{O}. \quad [5]$$

Notwithstanding this fact, the amount of surface Cu^{2+} sites of the $CuCl_2$ phase is reduced by the sintering process. So, the overall effect on the catalyst activity cannot be foreseen.

5. CONCLUSIONS

XANES, EXAFS, EPR, and IR of adsorbed CO have allowed a demonstration of the fact that the ethylene

oxychlorination reaction can be performed at 500 K in three separate steps: (i) reduction of $CuCl_2$ to more dispersed CuCl particles; (ii) oxidation of CuCl to give an oxychloride (Cu_2OCl_2 being a good candidate), with a partial sintering of the copper involved in the transformation; and (iii) closure of the catalytic circle by rechlorination with HCl, which restores the original $CuCl_2$. By increasing the reaction temperature, the rechlorination involves also the Cu^{2+} of the surface aluminate phase and leads to a severe sintering of the $CuCl_2$ particles.

ACKNOWLEDGMENTS

We are strongly indebted to E. Giamello and G. Turnes Palomino for fruitful discussion and to F. Bonino and A. Gabanotto for their relevant and friendly support during EXAFS measurements.

REFERENCES

1. Garilli, M., Fatutto, P. L., and Piga, F., *Chim. Ind.* **80**, 333 (1998).
2. (a) McPherson, R. W., Starks, C. M., and Fryar, G. J., *Hydrocarbon Process.* **58**, 75 (1979); (b) Naworski, J. S., and Evil, E. S., *Appl. Ind. Catal.* **1**, 239 (1983).
3. Mross, W. D., *Catal. Rev. Sci. Eng.* **25**, 591 (1983).
4. (a) Arcoya, A., Cortes, A., and Seoane, X. L., *Can. J. Chem. Eng.* **60**, 55 (1982); (b) Vetrivel, R., Rao, K. V., Seshan, K., Krishnamurthy, K. R., and Prasada Rao, T. S. R., *Proc. 9th Int. Congr. Catal.* Calgary **5**, 1766 (1988).
5. Leofanti, G., Padovan, M., Garilli, M., Carmello, D., Zecchina, A., Spoto, G., Bordiga, S., Turnes Palomino, G., and Lamberti, C., *J. Catal.* **189**, 91 (2000).
6. Leofanti, G., Padovan, M., Garilli, M., Carmello, D., Marra, G. L., Zecchina, A., Spoto, G., Bordiga, S., and Lamberti, C., *J. Catal.* **189**, 105 (2000).
7. (a) Casali, G., Cremaschi, B., Spoto, G., Carmello, D., Lamberti, C., Leofanti, G., and Zecchina, A., presented at EUROPA-CAT-4, Rimini (I), 5–10, September (2000); (b) Garilli, M., Carmello, D., Cremaschi, B., Leofanti, G., Padovan, M., Zecchina, A., Spoto, G., Bordiga, S., and Lamberti, C., presented at ICC-11, Granada (S), 9–14 July (2000), *Stud. Surf. Sci. Catal.* **130**, 1917 (2000).
8. Leofanti, G., Marsella, A., Cremaschi, B., Garilli, M., Marra, G. L., Zecchina, A., Spoto, G., Bordiga, S., Fisicaro, P., Berlier, G., Prestipino, C., Casali, G., and Lamberti, C., *J. Catal.* **202**, 279 (2001).
9. Naworski, J. S., and Evil, E. S., *Appl. Ind. Catal.* **1**, 239 (1983).
10. Allen, J. A., *J. Appl. Chem.* **12**, 406 (1962).
11. Carrubba, R. V., and Spencer, J. L., *Ind. Eng. Chem. Proc. Develop.* **9**, 414 (1970).
12. Arganbright, R. P., and Yates, W. F., *J. Org. Chem.* **27**, 1205 (1962).
13. Rollins, K., and Sermon, P. A., *J. Chem. Soc. Chem. Commun.* 1171 (1986).
14. Dmitrieva, M. P., Bahshi, Yu. M., and Gel'bshtein, A. I., *Kinet. Katal.* **31**, 894 (1990).
15. (a) Michalowicz, A., *J. Phys. IV* **7**, C2-235 (1997); (b) Michalowicz, A., Ph.D. thesis. Université Paris Val de Marne, 1990.
16. (a) Lytle, F. W., Sayers, D. E., and Stern, E. A., *Physica B* **158**, 701 (1989); (b) Durham, P. J., *in* "X-Ray Absorption" (D. C. Koningsberger and R. Prins, Eds.), p. 53. Willey, New York, 1988.
17. Lamberti, C., Bordiga, S., Salvalaggio, M., Spoto, G., Zecchina, A., Geobaldo, F., Vlaic, G., and Bellatreccia, M., *J. Phys. Chem. B* **101**, 344 (1997).
18. Burns, P. C., and Hawthorne, F. C., *Am. Mineral.* **78**, 187 (1993).
19. Restori, R., and Schwarzenbach, D., *Acta Cryst. B* **42**, 201 (1986).
20. (a) Strauss, S. H., *J. Chem. Soc. Dalton Trans.* 1 (2000); (b) Lupinetti, A. J., Strauss, S. H., and Frenking, G., *Prog. Inorg. Chem.* **49**, 1 (2001); (c) Zecchina, A., Scarano, D., Bordiga, S., Spoto, G., and Lamberti, C., *Adv. Catal.* **46**, 265 (2001).
21. Hadjiivanov, K., and Knözinger, H., *J. Catal.* **191**, 480 (2000).
22. Turnes Palomino, G., Fisicaro, P., Bordiga, S., Zecchina, A., Giamello, E., and Lamberti, C., *J. Phys. Chem. B* **104**, 4064 (2000).
23. Morterra, C., Giamello, E., Cerrato, G., Centi, G., and Perathoner, S., *J. Catal.* **179**, 111 (1998).
24. Arpe, R., and Müller-Buchbaum, B., *Z. Naturforsch. B* **32**, 380 (1977).